



Measurement of Polarization of the $\Upsilon(1S)$ and $\Upsilon(2S)$

The D0 Collaboration

URL: <http://www-d0.fnal.gov>

(dated: July 13, 2007)

Abstract

We present a study of the polarization of the $\Upsilon(1S)$ and $\Upsilon(2S)$ using a sample of 1.3 fb^{-1} of data collected by the D0 experiment in 2002–2006 during Run II of the Fermilab Tevatron. The polarization parameter $\alpha = (\sigma_T - 2\sigma_L)/(\sigma_T + 2\sigma_L)$ where σ_T and σ_L are the transverse and longitudinal polarized components of the cross section is measured as a function of transverse momentum (p_T) for the $\Upsilon(1S)$ and $\Upsilon(2S)$. Significant longitudinal polarization that is dependent on p_T is observed for the $\Upsilon(1S)$ that is inconsistent with QCD predictions. No contradictions to the NRQCD predictions for $\Upsilon(2S)$ are observed.

Preliminary Results for EPS2007

I. INTRODUCTION

The non-relativistic QCD (NRQCD) factorization approach has been developed to describe the inclusive production and decay of quarkonium [1] including high transverse momentum (p_T) S -wave charmonium production at the Tevatron [2]. The theory introduces several nonperturbative color-octet matrix elements (ME). These ME's are universal and fitted to data at the Tevatron. The universality of the ME has been tested in various experimental situations [3]. A remarkable prediction of the NRQCD is that the S -wave quarkonium produced in the $p\bar{p}$ collision should be transversely polarized at sufficiently large p_T [4]. This prediction is based on the dominance of gluon fragmentation in quarkonium production at large p_T [2] and on the approximate heavy-quark spin symmetry of NRQCD [1]. Measurements of the polarization of prompt J/ψ by the CDF Collaboration do not confirm this prediction [5].

A convenient measure of the polarization is the variable

$$\alpha = (\sigma_T - 2\sigma_L)/(\sigma_T + 2\sigma_L),$$

where σ_T and σ_L are the transverse and longitudinal polarized components of the cross section. If we consider the decays of quarkonia to a lepton, anti-lepton pair, then the angular distribution is given by

$$\frac{dN}{d(\cos\theta^*)} \propto 1 + \alpha \cos^2\theta^*, \quad (1)$$

where θ is the angle of the positive lepton in the center of mass frame with respect to the momentum direction of the decaying quarkonium in the lab system.

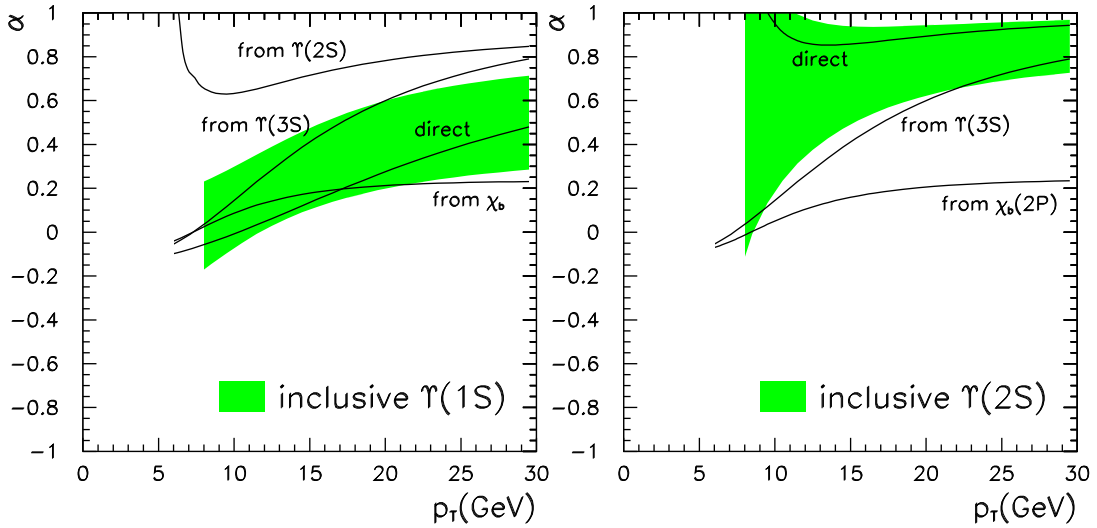


Figure 1: Theoretical predictions of the p_T -dependence of α for the Upsilon system [6]

Quantitative calculations of the polarization for inclusive $\Upsilon(nS)$ mesons are carried out [6] by using the ME for direct bottomonium production determined from an analysis of data at the Tevatron [7]. The theoretical predictions [6] for the polarization of the $\Upsilon(nS)$ are shown in Fig. 1. It is also predicted that the transverse polarization of $\Upsilon(1S)$ should increase steadily with p_T

for p_T greater than about 10 GeV and that the $\Upsilon(2S)$ and $\Upsilon(3S)$ should be even more strongly transversely polarized. The kt -factorization model [8], developing a semi-hard approach, predicts a longitudinal polarization at $p_T > 5$ GeV.

In this connection the experimental measurement of the Υ polarization is an crucial test of two theoretical approaches to parton dynamics in QCD.

II. SAMPLE SELECTION

The D0 detector is a general purpose spectrometer and calorimeter [9]. The tracking system of the detector includes a silicon microstrip tracker (SMT) and a central fiber tracker (CFT), both located within a 2 T superconducting solenoidal magnet. The SMT has 800,000 individual strips, with typical pitch of 50 – 150 μm , and a design optimized for tracking and vertexing capability at pseudorapidities of $|\eta| < 2.5$. The CFT has eight coaxial barrels, each supporting two doublets of scintillating fibers of 0.835 mm diameter, one doublet being parallel to the collision axis, and the other alternating by $\pm 3^\circ$ relative to the axis. For an identification of electronic and hadronic components there is the liquid argon calorimeter. A muon system resides beyond the calorimeter, and consists of a layer of tracking detectors and scintillation trigger counters before 1.8 T toroids, followed by two similar layers after the toroids. Luminosity is measured using scintillator arrays located in front of the end calorimeter cryostats, covering $2.7 < |\eta| < 4.4$. Trigger and data acquisition systems are designed to accommodate the high luminosities of the Tevatron Run II. Based on information from tracking, calorimetry, and muon systems, the output of the first two levels of the trigger is used to limit the rate for accepted events to ≈ 1.5 kHz and ≈ 800 Hz respectively,. The third and final level of the trigger, which has access to all the event information, uses software algorithms and a computing farm to reduce the output rate to ≈ 100 Hz, which is written to tape.

The data set used for this analysis includes approximately 1.3 fb^{-1} of integrated luminosity accumulated by the D0 detector between April 2002 and the end of 2006. Only the information from muon and tracking systems was used.

We selected events where the Υ decayed into two muons. Muons were identified using standard D0 criteria. For this analysis muons were required to have hits in 3 muon chambers, to have an associated track in the central tracking system with hits in both the SMT and CFT, and to have transverse momentum $p_T^\mu > 3.5$ GeV. The distribution of the dimuon invariant mass after these selection criteria is shown in Fig. 2a. We observed about 420,000 Upsilon candidates when fitting to these peaks as described below.

In this analysis only events that passed dimuon triggers were included in the final sample (see Fig. 2b). Approximately 40% of the $\Upsilon(nS)$ are removed by the trigger selection. The invariant mass resolution at these high mass values is not sufficient to resolve all the $\Upsilon(nS)$ signals; only the $\Upsilon(1S)$ peak is clearly resolved.

D \emptyset , Run 2 Preliminary, 1.3 fb⁻¹

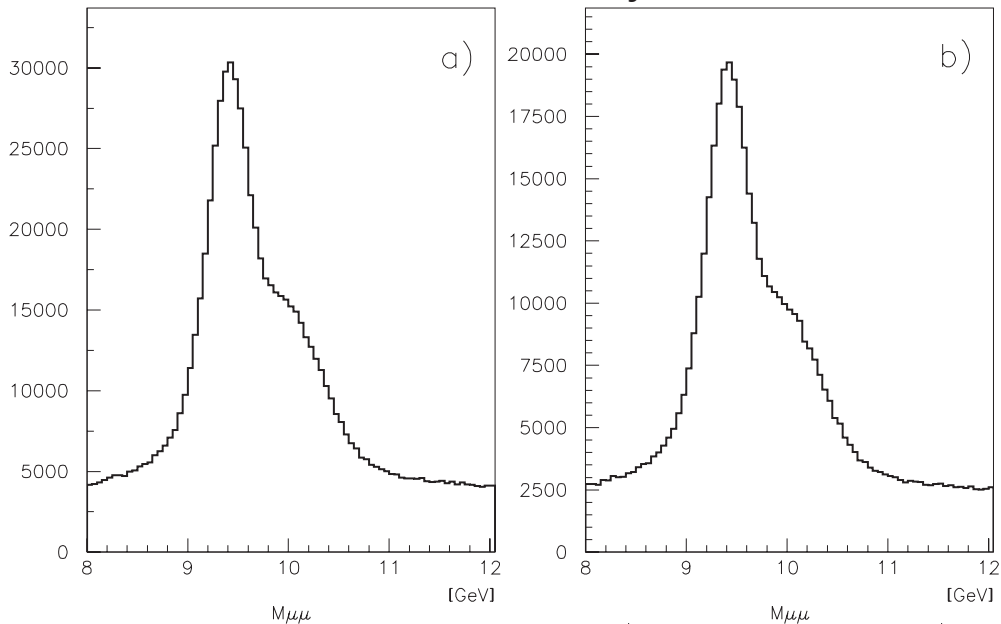


Figure 2: The dimuon invariant mass distribution after a) event selection and b) after event and trigger selection.

III. MONTE CARLO SIMULATION OF THE Υ SYSTEM

Monte Carlo samples of 860,000 $\Upsilon(1S)$ events and 900,000 $\Upsilon(2S)$ were generated using the PYTHIA [10] event generator and then passed through a GEANT [11] simulation of the D0 detector. Each event is required to have two muons satisfying $p_T^\mu > 2.0$ GeV and $|\eta_\mu| < 5$. The simulated events are then required to pass the same selection criteria as the data sample.

IV. SIGNAL EXTRACTION

We fit the dimuon invariant mass distribution in several intervals of p_T for a set of $|\cos\theta^*|$ bins. A previous study of the Υ cross-section by the D0 experiment [12] shows that a double Gaussian function is required to model the mass distribution of the upsilon. Investigation of the Upsilon Monte Carlo requires a more complicated parametrization of the invariant mass distribution for some of the $|\cos\theta^*|$ bins, where we observe an asymmetric mass distribution. Two parameterizations of the mass distribution were used. The first is a double Gaussian with the following free parameters

- N - the total number of $\Upsilon(nS)$ events ;
- Δ_c - the shift of the peak position relative to the PDG value [13];

- σ_1 - the resolution of the 1st Gaussian;
- $\delta_{N_2} = N_2/N$, where N_2 is the number of Υ events under the 2nd Gaussian;
- $\delta_{\sigma_2} = \sigma_2/\sigma_1$; where σ_2 is the resolution of the 2nd Gaussian.

The second parameterization was the sum of three Gaussians with one additional free parameter:

- Δ_l - the shift of the 3rd Gaussian relative to the peak position, defined by the common position of the 1st and 2nd Gaussians.

The number of Υ events under the 3rd Gaussian was fixed to be $0.25N$ and the resolution set to $\sigma_3 = 2.2\sigma_1$. These ratios were defined from MC.

Figure 3 shows an example of a fit to the mass distribution for a single p_T and $|\cos\theta^*|$ bin using the two and three Gaussian parameterizations. The signal consists of three mass peaks, the $\Upsilon(1S)$, $\Upsilon(2S)$ and $\Upsilon(3S)$ where the mass differences were fixed to the measured values [13]. The background was modeled with a convolution of an exponential and a polynomial functions. The degree of the polynomial was chosen between 1 to 6 depending on the complexity of the shape of the background.

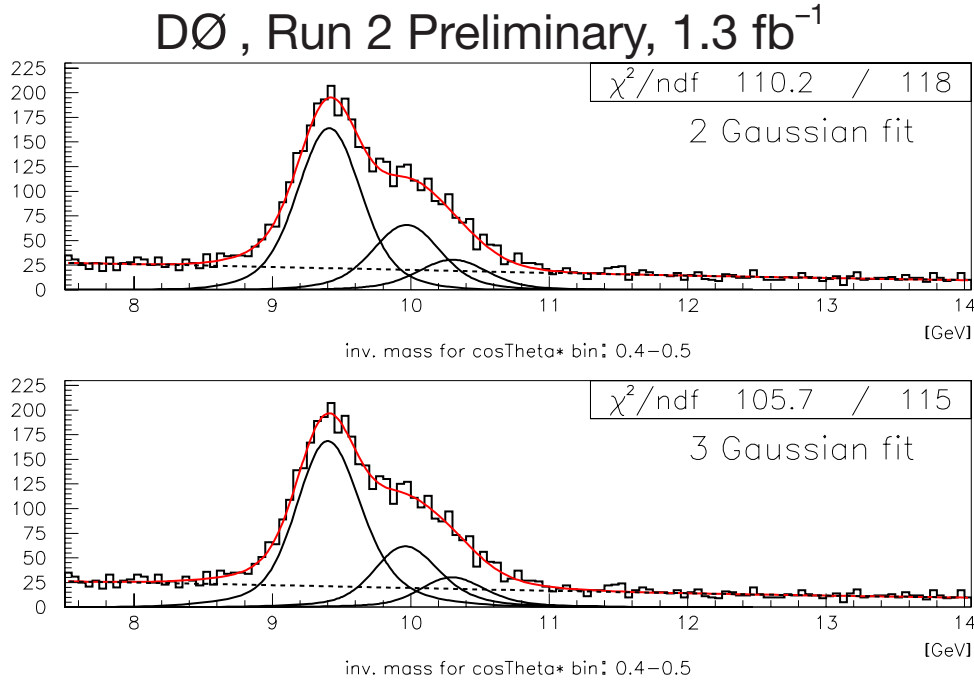


Figure 3: The Υ signal for $0.4 < |\cos\theta^*| < 0.5$, $10 < p_T^\Upsilon < 15$ GeV (black curves: $\Upsilon(1S) - \Upsilon(3S)$, dashed line: background, red line: sum of the Upsilon signals).

The data were divided into different bins in p_T^Υ and $|\cos\theta^*|$. For each of these bins the number of $\Upsilon(1S)$ and $\Upsilon(2S)$ events were extracted from the mass distribution. The resulting angular distributions are plotted for each of the p_T^Υ bins in Fig. 4. The number of $\Upsilon(3S)$ were insufficient to extract angular distributions.

DØ, Run 2 Preliminary, 1.3 fb⁻¹

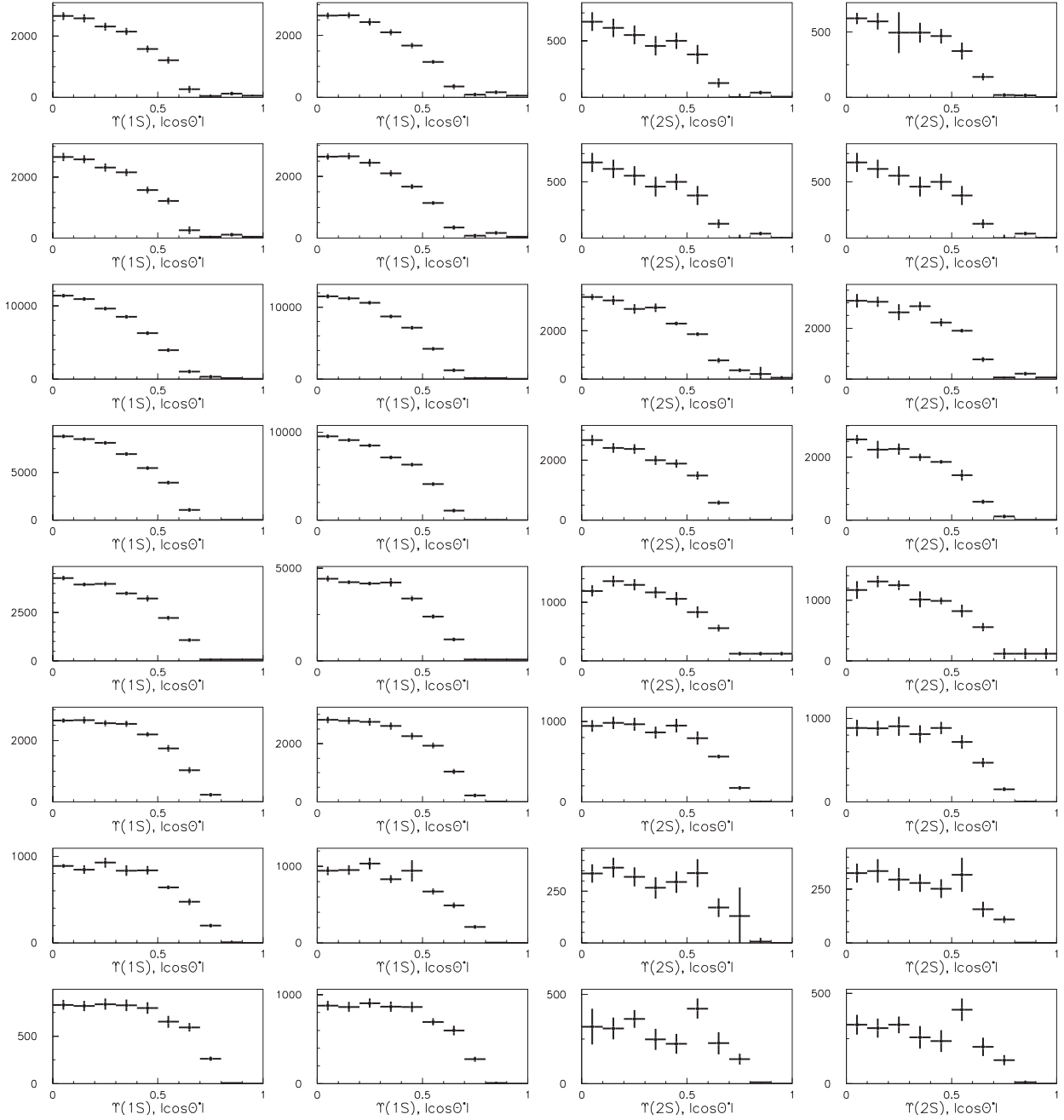


Figure 4: $|\cos\theta^*|$, data (rows from top to bottom: $0 < p_T^x < 1$, $1 < p_T^x < 2$, $2 < p_T^x < 4$, $4 < p_T^x < 7$, $7 < p_T^x < 10$, $10 < p_T^x < 15$, $14 < p_T^x < 20$ GeV, $p_T^x > 15$ GeV; columns from left to right show different fits: 2 Gaussians, 3 Gaussians, 2 Gaussians, 3 Gaussians).

V. CALCULATION OF α

The following algorithm was used to determine the parameter α for a given bin:

1. Select the data for a specified p_T^Υ interval;
2. determine the $|\cos\theta^*|$ distribution by extracting the number of $\Upsilon(nS)$ events from the mass distribution;
3. select a matching MC sample in the same bin;
4. select a value of α and calculate the weight w_α , which will convert the initial MC $|\cos\theta^*|$ distribution with $\alpha = 0$ to a distribution with the chosen value of α ,
5. calculated the χ^2 value between the data and MC distributions;
6. Find the minimum of $\chi^2(\alpha)$ by repeating pp.4-5.

The PYTHIA simulation does not accurately produce the kinematic distributions of Upsilon production at the Tevatron (e.g., the p_T^Υ distribution). Figure 5 shows a comparison between several kinematic distributions for MC and data. Significant differences are observed in several of the variables.

Figure 5 shows a comparison between the $\Upsilon(1S)$ MC simulation and the data for a p_T^Υ bin for several kinematic variables. There is a significant disagreement for the Υ momentum, p_T^Υ , and $|\cos\theta^*|$ distributions. This disagreement is due to the production model used in PYTHIA.

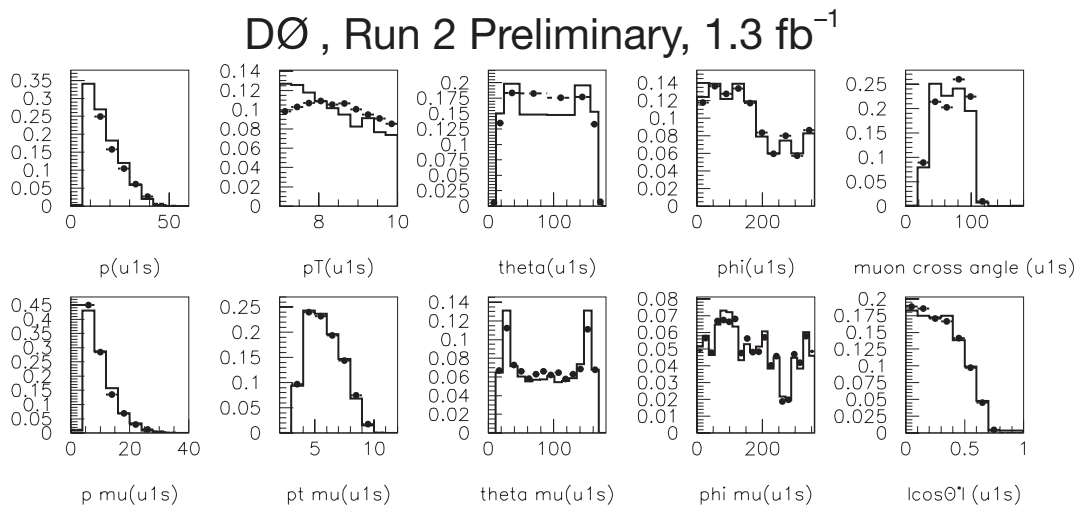


Figure 5: Comparison of data with reweighted MC (to $\alpha = -0.34$) providing the best χ^2 value for $7 < p_T^\Upsilon < 10$ GeV (Line: data, points: MC).

To correct the MC distributions we introduce additional weights to correct the Υ momentum distribution. Instead of the weight w_α in point 4 of our algorithm we use the weight $w = w_\alpha w_{p_T^\Upsilon} w_{p_T^\mu}$, where $w_{p_T^\Upsilon}$ and $w_{p_T^\mu}$ are weights to smooth the discrepancy between data and MC for distributions of p_T^Υ and p_T^μ . After this correction, for the example of Fig. 5, we obtain a new value of $\alpha = -0.42$ and good agreement between data and MC (Fig. 6) for the Upsilon and muon kinematic characteristics.

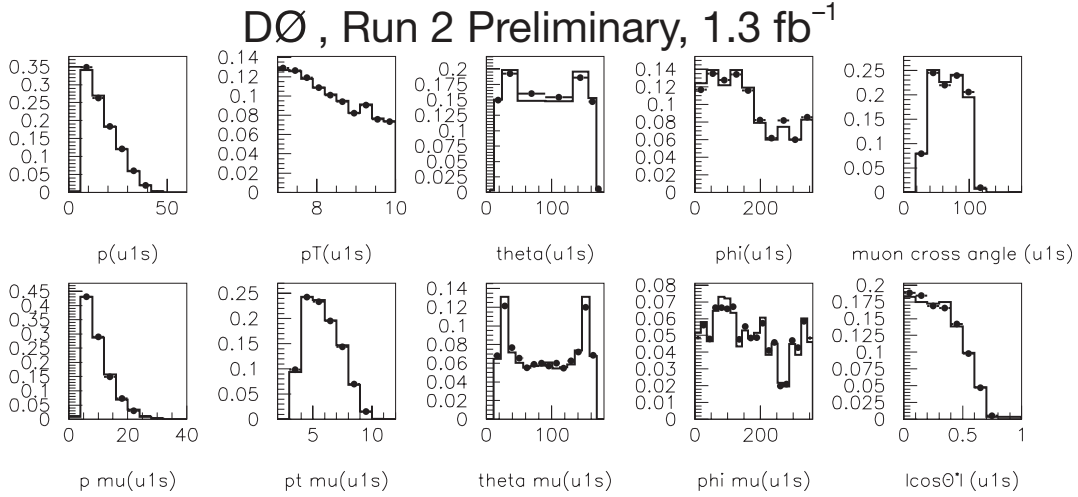


Figure 6: Comparison of data with reweighted MC (to $\alpha = -0.42$ and to Υ momentum distributions observed in data) providing the best χ^2 value for $7 < p_T^\Upsilon < 10$ GeV (line: data, points: MC).

VI. POLARIZATION OF $\Upsilon(1S)$

Figure 7 shows the dependence of α for $\Upsilon(1S)$ on p_T^Υ . The error bars show the sum in quadrature of the statistical and systematic uncertainties due to the parameterization of the background. The uncertainty in the background was estimated by varying the mass range of the fit and the degree of the polynomial used to parameterize the background.

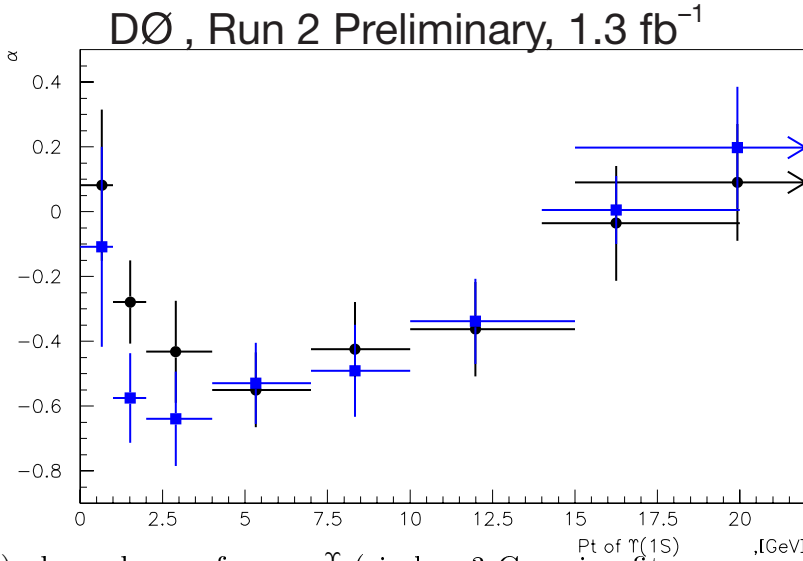


Figure 7: $\Upsilon(1S)$, dependence of α on p_T^Υ (circles: 3 Gaussian fit, squares: 2 Gaussian fit)

We observe a strong dependence of α on p_T^Υ .

VII. SYSTEMATIC UNCERTAINTIES

The systematic uncertainties of α for $\Upsilon(1S)$ are summarised in Table 1.

The systematic errors called "Signal Model" (see Table 1) was defined in each p_T interval as the difference between the average α of two signal fits used and their values.

The $\Upsilon(1S)$ polarization was calculated assuming that α is constant for a given p_T^Υ bin. To estimate the uncertainty due to this, the fitting procedure was reweighted using the observed dependence of α on p_T^Υ as shown in Fig. 7. The necessary correction are shown in Table 1 in the field "MC (no dependence on p_T^Υ)".

Figure 8 shows a comparison between the $|\cos\theta^*|$ distributions for MC simulations of the $\Upsilon(1S)$ and $\Upsilon(2S)$. There is a dependence in the $|\cos\theta^*|$ distributions on the mass. Our MC does not reproduce exactly the position of the Upsilon peak, which differs by about 40 MeV. The MC is then reweighted so that the Upsilon mass in the MC matches that of the data. The effect on the α distribution is estimated and included as "MC (shift of the Υ peak)".

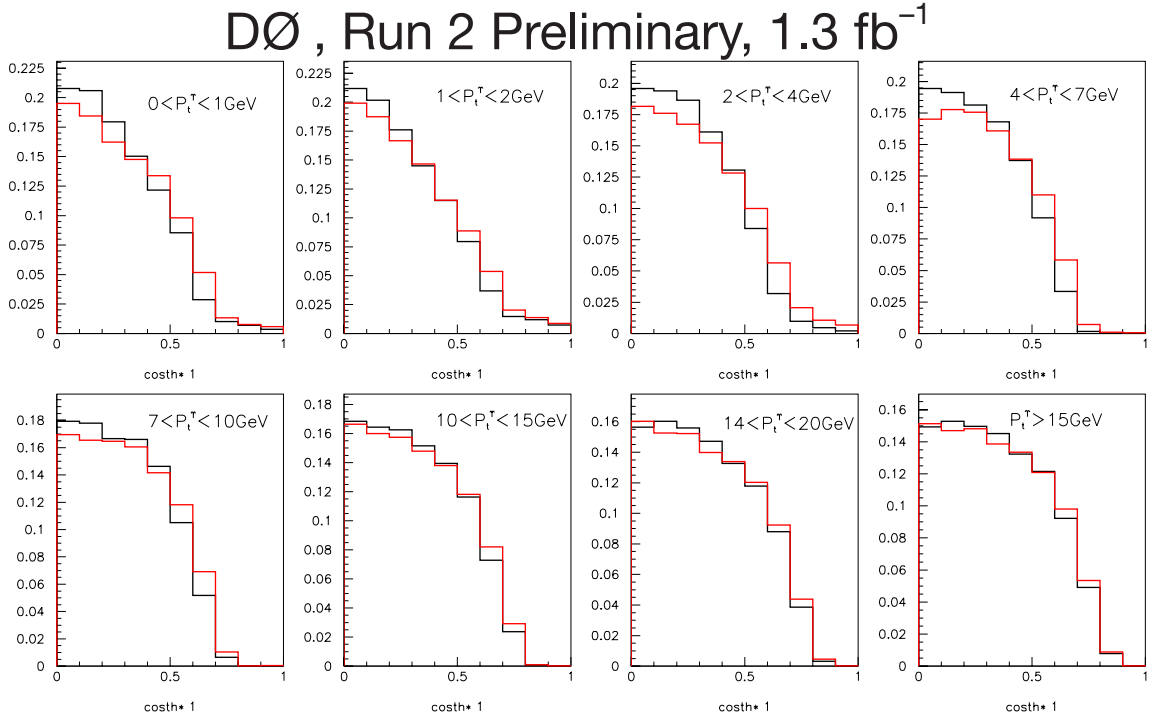


Figure 8: MC $|\cos\theta^*|$ distributions for $\Upsilon(1S)$ (black) and $\Upsilon(2S)$ (red).

At the moment we do not know exactly the accuracy of the simulation of the dimuon triggers used. Estimations give a value of about 5% for the uncertainty of trigger efficiency, which was used for the calculation of possible systematic errors shown in Table 1. More work on this effect is underway.

Table 1: Systematic errors of α

Source	p_T^Υ interval, [GeV]	Error
Background	all	0.04÷0.21 (included in stat. err.)
Signal Model	0 – 1	±0.09
	1 – 2	±0.15
	2 – 4	±0.10
	4 – 7	±0.01
	7 – 10	±0.03
	10 – 15	±0.01
	14 – 20	±0.02
	> 15	±0.05
MC (no dependence on p_T^Υ)	0 – 1	+0.02
	1 – 2	-0.03
	2 – 4	-0.03
	4 – 7	-0.02
	7 – 10	0.00
	10 – 15	-0.02
	14 – 20	+0.03
	> 15	+0.06
MC (shift of the Υ peak)	0 – 1	+0.06
	1 – 2	+0.05
	2 – 4	+0.01
	4 – 7	+0.01
	7 – 10	0.00
	10 – 15	+0.01
	14 – 20	-0.01
	> 15	0.00
MC (trigger efficiency)	0 – 1	±0.12
	1 – 2	±0.04
	2 – 4	±0.06
	4 – 7	±0.06
	7 – 10	±0.05
	10 – 25	±0.04
	14 – 20	±0.03
	> 15	±0.03

VIII. RESULTS

Figure 10 shows the resulting $\alpha(p_T)$ distribution for $\Upsilon(1S)$ (black circles). Error bars show the systematic and statistical uncertainties added in quadrature. Also plotted are the NRQCD prediction [6] (yellow band), and the two limits of the kt-factorization model [14] (magenta curves). The lower line corresponds to the quark-spin conservation hypothesis, and the another one to the

full quark-spin depolarization hypothesis. Also shown is the previous measurement by CDF for $|y| < 0.4$ [15] (green triangles). The CDF data are given in p_T intervals; the data is plotted at a point consistent with the p_T distribution observed by D0.

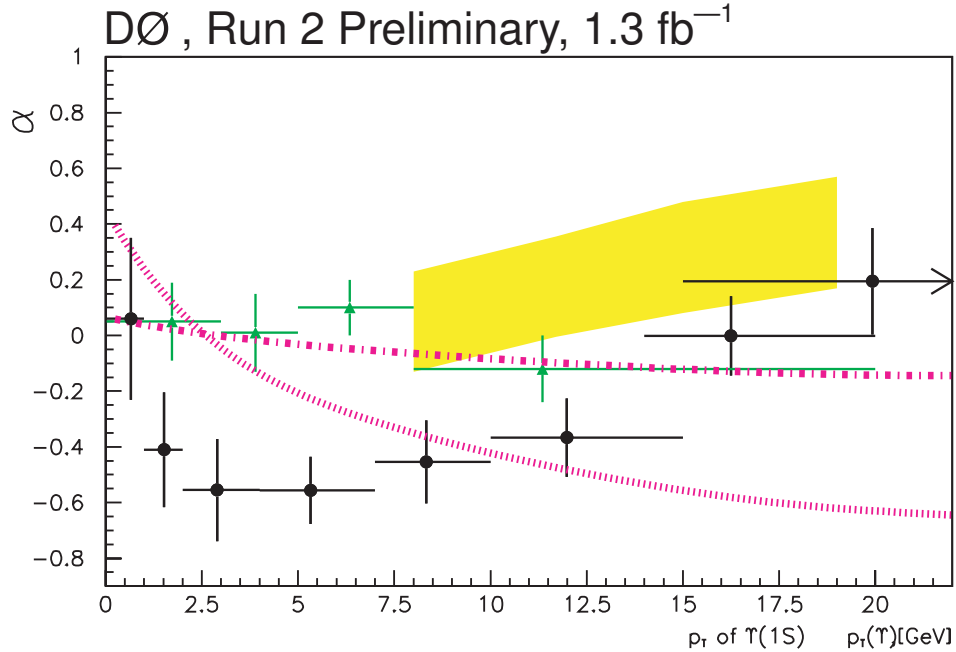


Figure 9: Dependence of α on p_T^x for inclusive $\Upsilon(1S)$. Black circles are our data. The yellow band is NRQCD predictions [6]. Magenta curves are two limit cases (see text) of the kt -factorization model [14]. Green triangles are the results of CDF experiment [15].

The same analysis, described in the previous chapters, was made and for $\Upsilon(2S)$ (see Figure 11). The yellow band shows theoretical predictions of NRQCD [6].

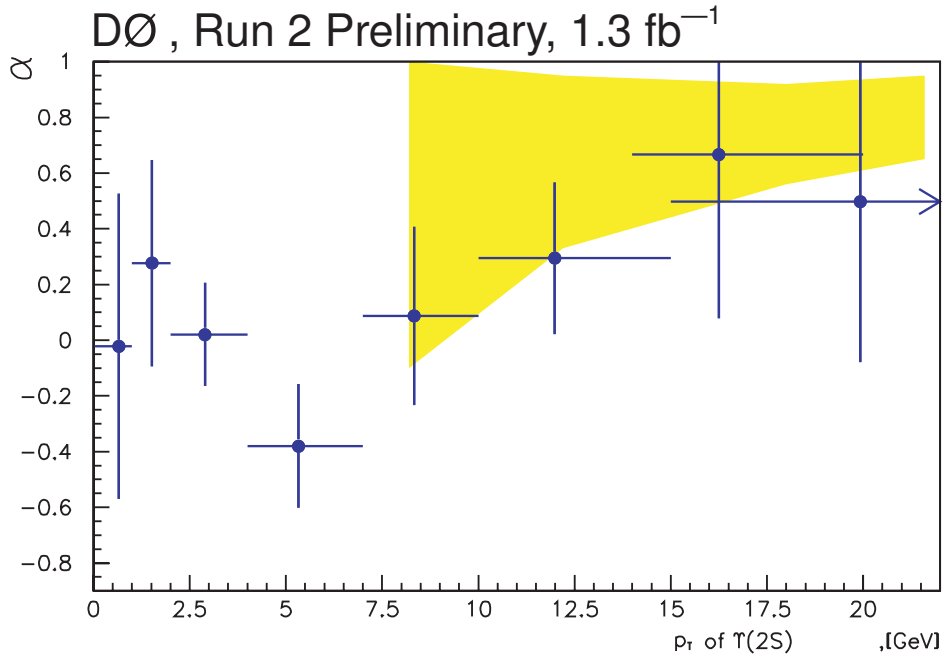


Figure 10: Dependence of α on p_T^x for inclusive $\Upsilon(2S)$. Blue circles are our data. The yellow band is NRQCD predictions [6].

IX. CONCLUSIONS

We have presented a measurement of the polarization of the $\Upsilon(1S)$ and $\Upsilon(2S)$ as a function of p_T from 0 to 20 GeV. Significant longitudinal polarization that is dependent on p_T is observed for the $\Upsilon(1S)$ that is inconsistent with QCD predictions. No contradictions to the NRQCD predictions for $\Upsilon(2S)$ are observed.

Acknowledgements

We thank the staffs at Fermilab and collaborating institutions, and acknowledge support from the DOE and NSF (USA); CEA and CNRS/IN2P3 (France); FASI, Rosatom and RFBR (Russia); CAPES, CNPq, FAPERJ, FAPESP and FUNDUNESP (Brazil); DAE and DST (India); Colciencias (Colombia); CONACyT (Mexico); KRF and KOSEF (Korea); CONICET and UBACyT (Argentina); FOM (The Netherlands); Science and Technology Facilities Council (United Kingdom); MSMT and GACR (Czech Republic); CRC Program, CFI, NSERC and WestGrid Project (Canada); BMBF and DFG (Germany); SFI (Ireland); The Swedish Research Council (Sweden); CAS and CNSF (China); Alexander von Humboldt Foundation; and the Marie Curie Program.

REFERENCES

- [1] G.T. Bodwin, E. Braaten, G.P. Lepage, Phys. Rev. **D51**, 1125 (1995); **55**, 5853(E) (1997)
- [2] E. Braaten, S. Fleming, Phys. Rev. Lett. **74**, 3327 (1995)
- [3] K. Anikeev *et al.*, Report of the working group on B physics at the Tevatron: 'Run II and beyond', hep-ph/0201071
- [4] P. Cho, M.B. Wise, Phys. Lett. **B346**, 129 (1995)
- [5] E. Braaten, B.A. Kniehl, J. Lee, Phys. Rev. **D62**, 094005 (2000); B.A. Kniehl, J. Lee, Phys. Rev. **D62**, 114027 (2000); T. Affolder (CDF Collaboration), *et al.*, Phys. Rev. Lett. **85**, 2886 (2000)
- [6] E. Braaten, J. Lee, Phys. Rev. **D63**, 071501 (R) (2001)
- [7] E. Braaten, A.K. Leibovich, S. Fleming, Phys. Rev. **D63** 094006 (2001)
- [8] J.R. Andersen *et al.*, Eur. Phys. J., C **35**, 67 (2004)
- [9] V. Abazov *et al.*, (D0 Collaboration), "The Upgraded D0 Detector", FERMILAB-PUB-05-341-E, Jul 2005. 142pp.
- [10] T. Sjöstrand *et al.*, Comput. Phys. Commun. **135**, 238 (2001).
- [11] Brun and F. Carminati, CERN Program Library Long Writeup W5013, 1993 (unpublished).
- [12] V. Abazov *et al.*, (D0 Collaboration), Phys. Rev. Lett. **94**, 232001 (2005)
- [13] W.-M. Yao *et al.*, Journal of Physics G **33**, 1 (2006).
- [14] S.P. Baranov, N.P. Zotov, HEP-PH/0707.0253
- [15] CDF Collaboration: D.Acosta *et al.*, Phys. Rev. Lett. **88**,161802 (2002)